Formation of cross-linked adducts between guanine and thymine mediated by hydroxyl radical and one-electron oxidation: a theoretical study

Vanessa Labet,[a] Christophe Morell,[a] André Grand,[a] Jean Cadet,[a] Paola Cimino[b] and Vincenzo Barone*[c]

Received 2nd April 2008, Accepted 17th June 2008
First published as an Advance Article on the web 24th July 2008
DOI: 10.1039/b805589k

The role of local geometric and stereo-electronic effects in tuning the preference for different cross-linked adducts between thymine and purinic bases has been analyzed by a computational approach rooted in density functional theory. Our study points out that G^T and T^G tandem lesions are produced according to the same mechanism as A^T and T^A intrastrand adducts, and in both cases purine^T adducts are preferred rather than the opposite sequences. Moreover, use of conceptual DFT tools allows the rationalization of the preferential occurrence of G^T and T^G tandem lesions in place of their A^T and T^A counterparts.

1. Introduction

Formation of intrastrand cross-links between the methyl group of thymine or 5-methylcytosine and the C8 atom of either adenine or guanine mediated by hydroxyl radical or one-electron oxidation is now well documented.[1–3] Adduct formation has been rationalized in terms of OH radical abstraction from the methyl group of either thymine (T) or 5-methylcytosine followed by the addition of the 5-(uracilyl)methyl or 5-(cytosyl)methyl radical to the C8 position of a vicinal purine base on the same DNA strand. The latter methyl radical can be generated by one-electron oxidation of either thymine or 5-methylcytosine, the resulting radical cation thus formed being susceptible to fast and efficient deprotonation on the methyl group.[4–6] The mechanism of the cross-link formation was inferred from the specific formation of the latter radicals by UV irradiation of photolabile 5-(phenylthiomethyl)-2′-deoxyuridine (or related 2′-deoxycytidine derivative) precursors,[7–9] once site-specifically inserted into oligonucleotides. Relevant information on the reactivity of the 5-(uracilyl)methyl radical with the adenine (A) and guanine (G) base either in the 3′- or the 5′-position was inferred from the measurement of the four possible A^T, T^A, G^T and T^G tandem base lesions[10] using a specific and sensitive high-performance liquid chromatography analytical tool coupled on line with a tandem mass spectrometry detector operating in the electrospray ionization mode. Thus it was found that the G^T adduct with the guanine located on the 5′-end of the strand is more efficiently generated in isolated DNA exposed to OH radical in oxygen-free aqueous solutions than the other T^G position isomer. It is also noteworthy that the A^T and T^A cross-links are produced in lower yields. Evidence has been recently provided for the formation of G^T tandem lesions in DNA exposed in aerated aqueous solution to the Cu(II)/H_2O_2/ascorbate oxidizing system.[11] More recently, evidence has been provided for the radiation-induced formation of G^T tandem base lesion in the DNA of human HeLa cells.[11] Despite the low yield of the cross-link that was shown to be generated, this clearly emphasizes the biological relevance of such tandem base lesions, whose mutagenic features have been also assessed through DNA polymerase studies.[11–13] It has also been shown that G^T and related 5-methycytosine cross-link were substrates for the *E. coli* UvrABC nuclease, an enzyme removing bulky lesions by the nucleotide excision repair pathway.[14] The present work constitutes an extension to G^T and T^G intrastrand cross-links of a previous theoretical study on the mechanism of formation of A^T and T^A tandem base lesions.[15]

2. Computational methods

All the calculations were carried out using the Gaussian 03 package[16] at the B3LYP/6-31G(d,p)[17] level. After full geometry optimization, the different stationary points were characterized as either minima or transition states by calculating the harmonic vibrational frequencies. Zero-point energies (ZPEs) and thermal contributions to thermodynamic functions and activation parameters were computed from these structures and harmonic frequencies by using the rigid rotor/harmonic oscillator approximation and the standard expressions for an ideal gas in the canonical ensemble at 298.15 K and 1 atm.

Since a previous study[15] on A^T and T^A tandem lesions showed that solvent effects did not play a significant role in the reaction, all calculations were made in the gas phase.

3. Results and discussion

In analogy with the formation of the A^T and T^A tandem base lesions, the reactions leading to the formation of the G^T and T^G adducts begin with the homolytic cleavage of a C–H bond on the methyl group of a thymine residue that gives rise to the 5-(uracilyl)methyl radical (R). Subsequent reaction of the latter radical with a vicinal guanine on either the 3′- or 5′-end leads to the formation of stable adducts characterized by a covalent bond between the thymine -CH_2 group and the C8 atom of the purine base. It is noteworthy that a strong sequence effect tunes the formation of the G^T and T^G adducts. Thus it was found

[a]*Laboratoire "Lésions des Acides Nucléiques", INAC/SCIB, UMR-E 3 (CEA/UJF), CEA-Grenoble, 17 rue des Martyrs, 38054, Grenoble cedex 9, France*
[b]*Dipartimento di Scienze Farmaceutiche, Università di Salerno, Via Ponte don Melillo, 84084, Fisciano, Salerno, Italy*
[c]*IPCF-CNR Via G. Moruzzi, 156124, Pisa, Italy. E-mail: baronev@unina.it*

that there is a 4-fold preferential formation of the tandem lesion in the 5′-(guanine-thymine)-3′ sequence compared to the reversed one. This proportion is similar to the one found when adenine is substituted with guanine. However, compared to A^T and T^A, the G^T and T^G tandem base lesions are produced with higher efficiency.

The systems chosen for the rationalization of the reaction under investigation are the two dinucleoside monophosphates (5′-GT-3′ and 5′-TG-3′) shown in Scheme 1. They include the two nucleic bases [guanine (G) and thymine (T)] each covalently attached to a sugar residue, namely the 2-deoxyribose, together with the phosphodiester bridge connecting the two residues. These systems are able to account for all the local interactions supposed to play a role in tuning the reaction mechanism.

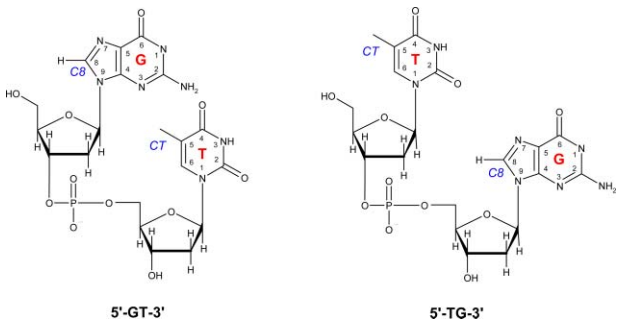

Scheme 1 Structures of the studied dinucleoside monophosphates 5′-**GT**-3′ and 5′-**TG**-3′.

The elimination of a hydrogen atom from the methyl group of thymine leads to the radical species located on the -CH_2 group (**R-GT** and **R-TG**) which are the starting reactive components of our mechanistic investigation (see Scheme 2).

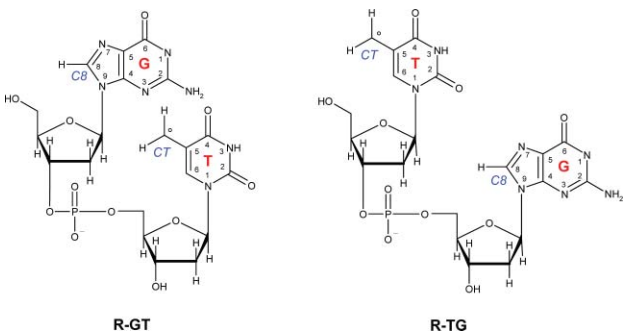

Scheme 2 Structures of the radical species **R-GT** and **R-TG**.

Full geometry optimization of the **R-GT** and **R-TG** systems leads to a distance between the two carbon atoms involved in the formation of the covalent link between the two bases of 7.32 Å and 3.73 Å, respectively. We may note that the distances thus calculated are different from the experimental values, for which the two concerned carbons are separated by 6.30 Å when the guanine is located at the 3′-extremity, and 3.58 Å when it is placed at the 5′-extremity. This is due to the lack of constraint introduced by the DNA sequence. Nevertheless, in our theoretical study on the formation of an intrastrand crosslink between thymine and adenine,[15] it has been shown that this model is sufficient to obtain a realistic mechanism for this kind of reaction.

In the following, we first analyze the mechanisms of the G^T and T^G tandem lesions (the final products are shown in Scheme 3) separately and then we compare them. In a final subsection the comparison will be extended to the previous studies aimed at investigating the reactivity of 5-(uracilyl)methyl radical with vicinal adenine.

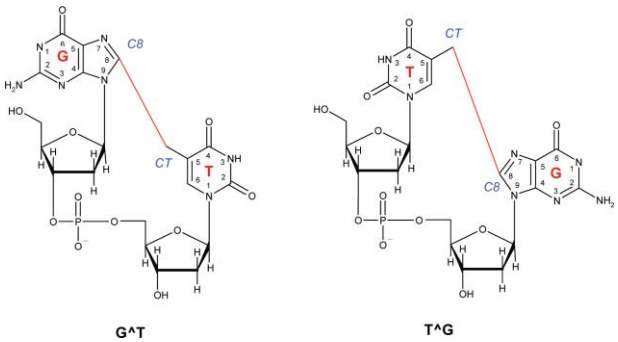

Scheme 3 Structures of the G^T and T^G tandem lesions.

3.1 G^T tandem lesion

The stepwise pathway for the reaction that is initiated by the **R-GT** radical can be described in terms of an addition–elimination mechanism characterized by two successive steps: the formation of a bond between the C8 atom of guanine and the methyl carbon CT of thymine, followed by the breaking of the C8–H8 bond, with the consequent release of a hydrogen atom.

The transition state (**TS1-GT**, Fig. 1) governing the first step is characterized by the incipient tetrahedral character of C8 (sp^2 hybridization in **R-GT** and sp^3 hybridization in the first intermediate); this is accompanied by the lengthening of the N7–C8 bond (to 1.350 Å), which is evolving from a double to a single bond, and by a shortening of the distance between CT and C8 to 2.131 Å. This transition state is very similar to the corresponding one (**TS1-AT**[15]) when adenine replaces guanine,

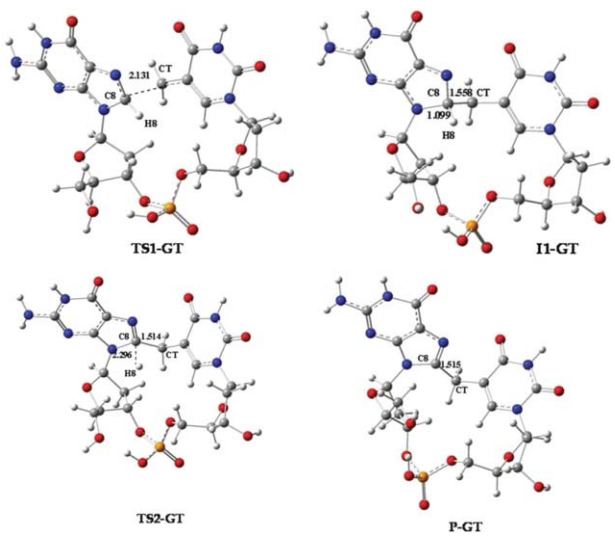

Fig. 1 Optimized structures of: transition state **TS1-GT**, intermediate **I1-GT**, transition state **TS2-GT** and product **P-GT** (the distances are in Å).

Table 1 Thermodynamic and kinetic parameters for the formation of the G^T tandem lesion under standard conditions (298.15 K, 1 atm) in the gas phase computed at the B3LYP/6-31G(d,p) level

	TS1-R	I1-R	TS2-I1	P-I1	P-R
ΔE/kcal mol^{-1}	+17.3	+1.6	+39.6	+39.5	+41.1
$T\Delta S$/kcal mol^{-1}	−6.4	−5.8	−0.8	+7.5	+1.7
ΔG/kcal mol^{-1}	+23.8	+7.4	+40.3	+32.6	+40.0

where the distances N7–C8 and CT–C8 were 1.377 Å and 2.142 Å, respectively. This step ends with the formation of a relatively stable intermediate, **I1-GT** (Fig. 1), in which the C8–CT and C8–H8 bond lengths are 1.558 and 1.099 Å, and which presents similar features to **I1-AT**, where the C8–CT and C8–H8 distances were 1.560 and 1.093 Å.

The reaction proceeds toward a second transition state (**TS2-GT**, Fig. 1) issuing from the breaking of the C8–H8 bond of guanine; this is characterized by a distance of 2.296 Å, which is longer than the corresponding distance in **TS2-AT**, which was only 1.916 Å. Finally, the reaction leads to the G^T tandem lesion observed experimentally (**P-GT**, Fig. 1). The energetics of all the reaction steps are outlined in Fig. 2 and Table 1.

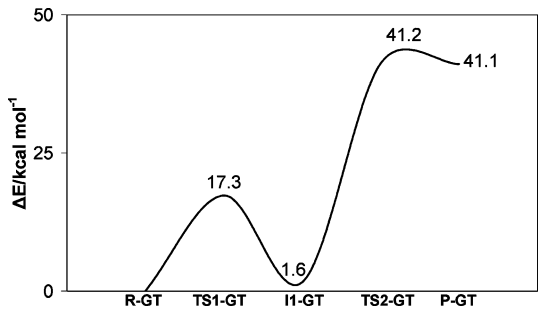

Fig. 2 Computed electronic energies (ΔE and $\Delta E^{\ddagger}$) of reaction steps involved in the formation of the G^T tandem lesion at the B3LYP/6-31G(d,p) level.

The energy barrier ($\Delta E^{\ddagger}_{(\text{TS1-GT}-\text{R-GT})}$) governing the first step is 17.3 kcal mol^{-1} (Fig. 2) and the corresponding free energy of activation ($\Delta G^{\ddagger}_{(\text{TS1-GT}-\text{R-GT})}$) was estimated to be 23.8 kcal mol^{-1} (Table 1), with a negative entropy contribution ($T\Delta S^{\ddagger}_{(\text{TS1-GT}-\text{R-GT})}$=−6.4 kcal mol^{-1}), probably related to the decreased flexibility of the whole structure. This first step appears much easier than in the case of the A^T tandem lesion, where the energy barrier was 41.5 kcal mol^{-1} with a corresponding free energy of activation of 44.2 kcal mol^{-1}.

The endoergity of this step is much reduced with respect to the corresponding reaction for the A^T tandem lesion (1.6 *vs.* 8.6 kcal mol^{-1}).

The second reaction step (Fig. 2, Table 1) is characterized by an activation free energy ($\Delta G^{\ddagger}_{(\text{TS2-GT}-\text{I1-GT})}$) of 40.3 kcal mol^{-1} ($\Delta G^{\ddagger}_{(\text{TS2-GT}-\text{R-GT})}$ = 47.7 kcal mol^{-1} with respect to the reactant), which is 3.6 kcal mol^{-1} higher than the corresponding barrier in the case of the A^T tandem lesion. The reaction free energy $\Delta G_{(\text{P-GT}-\text{I1-GT})}$) is 32.6 kcal mol^{-1} ($\Delta G_{(\text{P-GT}-\text{R-GT})}$ = 40.0 kcal mol^{-1} with respect to the reactant): thus the overall reaction is strongly endothermic (1.3 kcal mol^{-1} more than for A^T).

The rate-determining step is the breaking of the C8–H8 bond, with an associated activation energy ($\Delta E^{\ddagger}_{(\text{TS2-GT}-\text{R-GT})}$) of 41.2 kcal mol^{-1} with respect to the reactant ($\Delta G^{\ddagger}_{(\text{TS2-GT}-\text{R-GT})}$) = 47.7 kcal mol^{-1}). Similar values were previously found for the formation of A^T tandem lesion ($\Delta E^{\ddagger}_{(\text{TS2-AT}-\text{R-AT})}$) of 45.8 kcal mol^{-1} ($\Delta G^{\ddagger}_{(\text{TS2-AT}-\text{R-AT})}$) = 47.3 kcal mol^{-1}).

The much easier first step for G^T than for A^T increases the concentration of **I1-GT** respect to **I1-AT** for a same quantity of reactants **R-GT** and **R-AT**. Since there is a large quantity of radical species in the reaction medium which is able to react with the hydrogen H8 made available upon C–H bond breaking, the probability for intermediates **I1-GT** and **I1-AT** to produce **P-GT** and **P-AT** is much larger than the probability to return to the reactants, even if the energetic barrier to cross is higher. Since the strength of the C8–H bond is similar in both cases, the percentages of the final products (**P-GT** and **P-AT**) and of the intermediates (**I1-GT** and **I1-AT**) are the same. Thus, G^T tandem lesions are produced more efficiently than A^T ones. This is in agreement with the experimental observations.

3.2 T^G tandem lesion

The first step of the reaction of **R-TG** giving rise to T^G is the creation of a covalent link between the C8 of guanine and the CT of thymine. Then, the H8 atom does not leave from the intermediate species but is rather transferred to the thymine moiety, leading to a second intermediate, which in turn can evolve along different routes. Consequently, the reaction channel is more involved than the one producing the G^T tandem lesion.

The **R-TG** radical (Scheme 1), leads through the transition state **TS1-TG** (C8–CT = 2.105 Å, Fig. 3), to the intermediate **I1-TG** (Fig. 3) characterized by a covalent inter-base bond (C8–CT = 1.558 Å). The geometry of this transition state is very similar to the corresponding one involving adenine, in which the distance between C8 and CT was 2.158 Å.

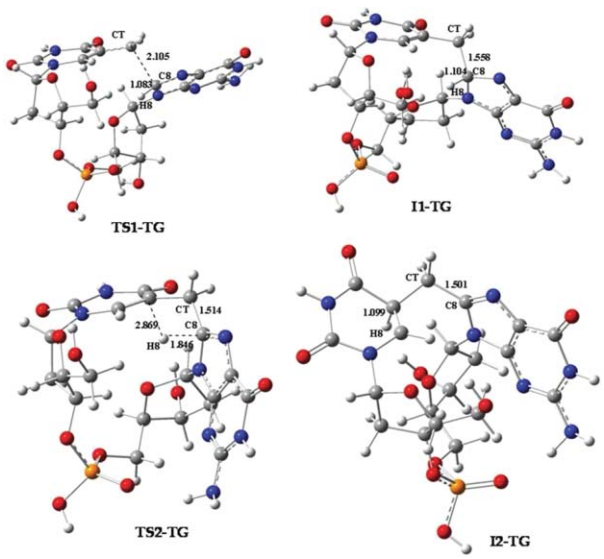

Fig. 3 Optimized structures of: transition state **TS1-TG**, intermediate **I1-TG**, transition state **TS2-TG**, and intermediate **I2-TG** (the distances are in Å).

The second step involves the cleavage of the C8–H8 bond, leading to a second intermediate (**I2-TG**, Fig. 3) in which H8 is attached to the C5 atom of thymine (C5–H8 = 1.099 Å), in

agreement with previous computational studies and experimental evidence.[18] In **TS2-TG** the distance between the H8 and the C5 atoms of thymine is longer than in the corresponding transition state (**TS2-TA**) involving adenine (2.869 *vs.* 2.593 Å).

Starting from **I2-TG**, two reaction channels are open. The first one corresponds to the homolytic cleavage of the C5–H8 bond, which leads through the transition state **TS3a-TG** (characterized by a C5–H8 distance of 1.881 Å, Fig. 4), to the formation of the T^G tandem lesion (**Pa-TG**, Fig. 4). The second channel corresponds, instead, to the cleavage of the C5–CT bond through the transition state **TS3b-TG** (characterized by a C5–CT bond length of 2.128 Å, Fig. 4) and subsequent formation of a dinucleoside involving uracil (U) and an 8-methylated guanine residue with a radical site at position 8 (**Pb-TG**, Fig. 4). This is expected to be a very reactive intermediate, which will spontaneously evolve, for instance by generating the neutral methylated guanine through reaction with hydrogen atoms that are available in the reaction medium. The energetics of all the reaction steps are reported in Fig. 5 and Table 2.

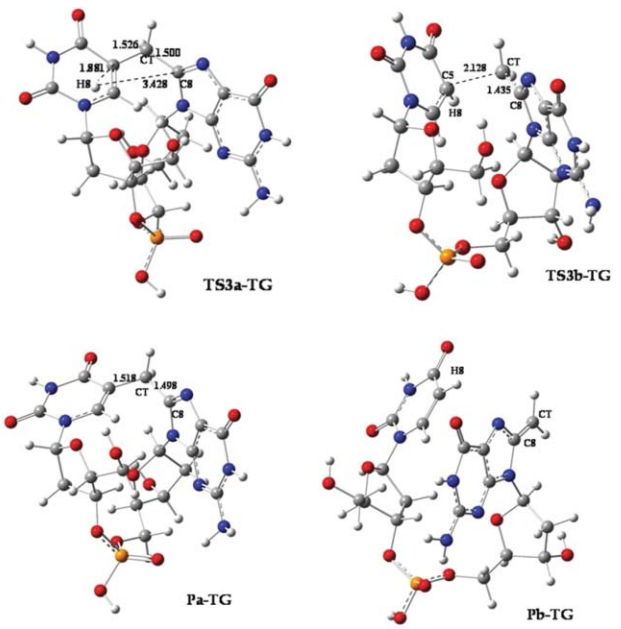

Fig. 4 Optimized structures of the transition states **TS3a-TG** and **TS3b-TG**, and products **Pa-TG** and **Pb-TG** (the distances are in Å).

The first step (Fig. 5, Table 2), corresponding to the formation of a covalent bond between the C8 atom of guanine and the methyl carbon CT of thymine, is ruled by an activation energy, $\Delta E^{\ddagger}_{(\text{TS1-TG}-\text{R-TG})}$, of 21.0 kcal mol^{-1} ($\Delta G^{\ddagger}_{(\text{TS1-TG}-\text{R-TG})}$= 21.7 kcal mol^{-1}), and a reaction energy, $\Delta E_{(\text{I1-TG}-\text{R-TG})}$, of 8.4 kcal mol^{-1} ($\Delta G_{(\text{I1-TG}-\text{R-TG})}$= 9.4 kcal mol^{-1}). Compared to the equivalent step involving adenine in place of guanine, the formation of this single

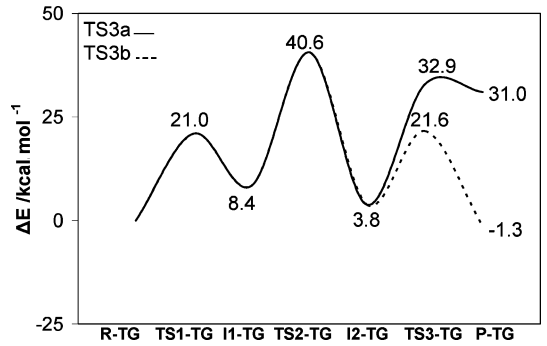

Fig. 5 Computed electronic energies (ΔE and $\Delta E^{\ddagger}$) of the reaction steps characterizing the mechanism of the T^G tandem lesion at the B3LYP/6-31G(d,p) level.

bond is about twice as easy when the purinic base is guanine. Indeed, the first step in the formation of the T^A tandem lesion was characterized by an activation energy, $\Delta E^{\ddagger}_{(\text{TS1-TA}-\text{R-TA})}$, of 39.3 kcal mol^{-1} ($\Delta G^{\ddagger}_{(\text{TS1-TA}-\text{R-TA})}$= 41.6 kcal mol^{-1}), and a reaction energy, $\Delta E_{(\text{I1-TA}-\text{R-TA})}$, of 12.1 kcal mol^{-1} ($\Delta G_{(\text{I1-TA}-\text{R-TA})}$= 12.6 kcal mol^{-1}). It is noteworthy that in both cases, although the entropic contribution is small, the kinetics of the reaction is slowed down. This is probably due to an increased rigidity of the transition state with respect to the radical reactant.

The second step (Fig. 5, Table 2) involves the breaking of the C8–H8 bond and the formation of the C5–H8 bond; the activation energy, $\Delta E^{\ddagger}_{(\text{TS2-TG}-\text{I1-TG})}$, is 32.2 kcal mol^{-1} ($\Delta G^{\ddagger}_{(\text{TS1-TG}-\text{R-TG})}$= 35.7 kcal mol^{-1}) and the reaction energy, $\Delta E_{(\text{I2-TG}-\text{R-TG})}$, 3.8 kcal mol^{-1} ($\Delta G_{(\text{I2-TG}-\text{R-TG})}$= 5.4 kcal mol^{-1}). Also this step is easier when the purinic base is a guanine instead of an adenine. However, the difference is less pronounced since the energetic parameters were $\Delta E^{\ddagger}_{(\text{TS2-TA}-\text{I1-TA})}$= 36.0 kcal mol^{-1}, $\Delta G^{\ddagger}_{(\text{TS1-TA}-\text{R-TA})}$= 37.2 kcal mol^{-1}, $\Delta E_{(\text{I2-TA}-\text{R-TA})}$= 11.0 kcal mol^{-1}, and $\Delta G_{(\text{I2-TA}-\text{R-TA})}$= 13.4 kcal mol^{-1}.

Then, the reaction can follow two alternative routes (Fig. 5, Table 2). The first one (**TS3a-TG**, **Pa-TG**) leads to the T^G tandem lesion through the cleavage of the C5–H8 bond with $\Delta E^{\ddagger}_{(\text{TS3a-TG}-\text{I2-TG})}$= 29.1 kcal mol^{-1} and $\Delta G^{\ddagger}_{(\text{TS3a-TG}-\text{I2-TG})}$= 29.3 kcal mol^{-1}. This energy barrier is higher than the equivalent one involved in the formation of the T^A tandem lesion ($\Delta E^{\ddagger}_{(\text{TS3a-TA}-\text{I2-TA})}$= 21.4 kcal mol^{-1}, and $\Delta G^{\ddagger}_{(\text{TS3a-TA}-\text{I2-TA})}$= 20.0 kcal mol^{-1}). The reaction energy is $\Delta E_{(\text{Pa-TG}-\text{I2-TG})}$= 27.2 kcal mol^{-1} ($\Delta G_{(\text{Pa-TG}-\text{I2-TG})}$= 23.2 kcal mol^{-1}). The entropic contribution is not negligible ($T\Delta S_{(\text{Pa-TG}-\text{I2-TG})}$= 4.6 kcal mol^{-1}), since a molecular system is transformed into a bimolecular one. However, it is lower than the related entropic contribution found when adenine replaces guanine ($T\Delta S_{(\text{Pa-TA}-\text{I2-TA})}$= 10.4 kcal mol^{-1}). This first route is overall strongly endothermic ($\Delta G_{(\text{Pa-TG}-\text{R-TG})}$= 28.6 kcal mol^{-1}). The second route, leading to the cleavage of the C5–CT bond, is characterized by $\Delta E^{\ddagger}_{(\text{TS3b-TG}-\text{I2-TG})}$= 17.8 kcal mol^{-1} and $\Delta E_{(\text{Pb-TG}-\text{I2-TG})}$=−5.1 kcal mol^{-1}. Since the latter step is

Table 2 Thermodynamic and kinetic parameters for the formation of the T^G tandem lesion under standard conditions (298.15 K, 1 atm) in the gas-phase computed at the B3LYP/6-31G(d,p) level

	TS1-R	I1-R	TS2-I1	I2-R	TS3a-I2	TS3b-I2	Pa-I2	Pb-I2
ΔE/kcal mol^{-1}	+21.0	+8.4	+32.2	+3.8	+29.1	+17.8	+27.2	−5.1
$T\Delta S$/kcal mol^{-1}	−0.8	−1.0	−3.5	−1.7	−0.2	+0.2	+4.6	+2.9
ΔG/kcal mol^{-1}	+21.7	+9.4	+35.7	+5.4	+29.3	+17.5	+23.2	−8.0

monomolecular, the entropic contribution is much smaller ($T\Delta S_{(\text{Pb-TG}-\text{I2-TG})}$= 2.9 kcal mol^{-1}) than in the first route ($T\Delta S_{(\text{Pa-TG}-\text{I2-TG})}$= 4.6 kcal mol^{-1}). The second route is overall slightly exothermic ($\Delta G_{(\text{Pb-TG}-\text{R-TG})}$=−2.6 kcal mol^{-1}). Thus, formation of uracil and methylated guanine is favored with respect to T^G tandem lesion from both kinetic and thermodynamic points of view.

The rate-determining step is the breaking of the C8–H8 bond, with an associated activation energy ($\Delta E^{\ddagger}_{(\text{TS2-TG}-\text{R-TG})}$) of 40.6 kcal mol^{-1} with respect to the reactant ($\Delta G^{\ddagger}_{(\text{TS2-TG}-\text{R-TG})}$)= 45.1 kcal mol^{-1}). Similar trends were previously found in the formation of A^T tandem lesion with an associated energy of activation ($\Delta E^{\ddagger}_{(\text{TS2-TA}-\text{R-TA})}$) of 48.0 kcal mol^{-1} ($\Delta G^{\ddagger}_{(\text{TS2-TA}-\text{R-TA})}$) = 49.8 kcal mol^{-1}).

In analogy with the remarks made in subsection 3.1, the fact that the energetic barrier associated with the first step is much lower when guanine replaces adenine explains why the T^G tandem base lesions are produced preferentially with respect to their T^A counterparts.

3.3 Discussion

The results of the preceding sections show that from both structural and energetic points of view, the mechanism of formation of G^T and T^G tandem lesions is very similar to that of A^T and T^A intrastrand adducts.

The C8–H8 bond breaking is always the rate-determining step, and the associated energetic barriers are similar. Yet, the first step, namely the formation of the covalent bond between the C8 atom of the purine and the CT carbon of -CH_2 of thymine, appears about twice as easy with guanine rather than with adenine. This difference favors the formation of **I1-GT** and **I1-TG** intermediates with respect to **I1-AT** and **I1-TA**, leading, in agreement with the experimental observations, to the formation of more tandem lesions involving guanine than adenine.

Use of conceptual DFT tools[19] can help to rationalize why the first step is easier when the purinic base is a guanine. The lower destabilization of the transition states **TS1-GT** and **TS1-TG** with respect to their counterparts, **TS1-AT** and **TS1-TA**, can be analyzed in terms of evolution of the chemical hardness along the corresponding reaction paths. Indeed, the so-called Principle of Maximum Hardness[20] states that molecular systems tend to be as hard as possible both in energy minima and in transition states. The $\Delta f(r)$ dual descriptor, introduced by Morell *et al.*,[21,22] characterizes the variations of the absolute hardness when the external potential changes, upon, for instance, approach of reactants during a bimolecular reaction. This descriptor has been calculated for the two purinic bases,[23] and the results are shown on Fig. 6. It can be seen that the $\Delta f(r)$ descriptor is positive for the C8 atom of adenine (red), whereas it is negative for the C8 carbon of guanine (green). This difference of sign indicates that the two bases do not share the same behavior towards an attack on their C8 atoms. When a site with a negative value of the dual descriptor ($\Delta f(r) < 0$), is attacked by an electrophilic reagent, the absolute hardness of the base will increase, whereas the hardness of the base will decrease if the attacking reagent is a nucleophile. Of course the situation is reversed when $\Delta f(r) > 0$. In the step we are interested in, the two bases are attacked at C8 by the electrophilic radical formed after abstraction by a hydroxyl

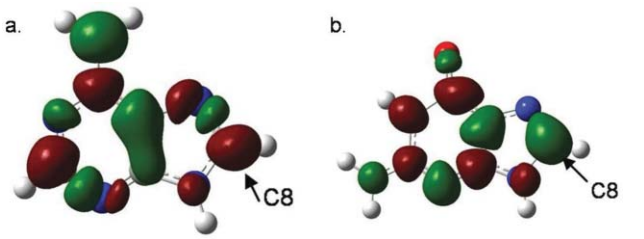

Fig. 6 $\Delta f(r)$ calculated at the B3LYP/6-311G(d,p) level for adenine (a) and guanine (b). The red areas correspond to positive values of $\Delta f(r)$, and the green to negative values.

radical of a hydrogen atom from the methyl group of thymine. Consequently, its interaction with C8 of adenine induces a decrease of the absolute hardness, which is unfavorable. In contrast, when the same radical attacks the C8 of guanine, there is an increase of the absolute hardness, which is favorable. This tendency can explain that **TS1-GT** and **TS1-TG** are harder than **TS1-AT** and **TS1-TA**, and consequently more stable.

Experimental studies reveal a larger amount of generated G^T tandem lesion with respect to the T^G sequence isomer, and on the basis of the present theoretical results this can be explained in the same way as the formation of T^A and A^T tandem lesions. The formation of G^T and T^G intrastrand adducts is determined by two factors: a geometric parameter linked to the DNA sequence, and a stereo-electronic factor related to the different reactivity of the dinucleoside monophosphates. Indeed, in the 5′-AT-3′ and 5′-GT-3′ sequences, after formation of the first intermediate, the reactive hydrogen H8 occupies a quite external position to the molecular surface of the nucleoside, and thus can be easily attacked by another radical species present in the reaction medium. In contrast, in the 5′-TA-3′ and 5′-TG-3′ sequences, the hydrogen points inside the molecular envelope, and its transfer to C5 is thus favored with respect to its extraction by external radicals. Moreover, it has been seen in this study, and in the previous one devoted to adenine,[15] that the selection between T^purine and purine^T tandem lesions occurs during the second reaction step, that is the C8–H8 breaking. From the R-purineT reactant, the C8–H8 breaking leads to a single product, the purine^T tandem lesion, which is less stable than the reactant. From the R-Tpurine, after transfer of H8 from C8 to C5, two products can be produced: the T^purine tandem lesion, which is also less stable than the reactant, and the methylated purine base, which is more stable. So the formation of this last product is favored with respect to the T^purine tandem lesion. This can explain why purine^T tandem lesions are experimentally generated more efficiently than their T^purine counterparts. The experimental observation of uracil among the reaction products would provide further support to this hypothesis.

4. Conclusions

The present theoretical study shows that G^T and T^G tandem lesions are produced according to the same mechanism as A^T and T^A intrastrand adducts. Therefore, the preferential formation of G^T and A^T tandem lesions with respect to the opposite sequence isomers can be explained in a similar way. Moreover, this study rationalizes the fact that G^T and T^G tandem lesions are produced preferentially compared to A^T and T^A ones. So

the use of a dinucleoside monophosphate model, with a lack of the constraints introduced by the DNA sequence, succeeds in a qualitative reproduction of the experimental observations concerning this kind of lesion. This confirms that the majority of the important interactions are relatively well described, and that the local stereo-electronic effects play the main role. Nevertheless, it could be interesting to perform QM/MM studies of larger fragments to have a proper description of the steric interactions involved.

References and notes

1 H. C. Box, E. E. Budzinski, J. D. Dawidzik, J. C. Wallace, M. S. Evans and J. S. Gobey, *Radiat. Res.*, 1996, **145**, 641–643.
2 H. C. Box, J. B. Dawidzik and E. E. Budzinski, *Free Radical Biol. Med.*, 2001, **31**, 856–868.
3 J. Cadet, T. Douki and J.-L. Ravanat, The Human Genome as a Target of Oxidative modification: Damage to Nucleic Acids, in *Redox–Genome Interactions in Health and Disease*, ed. J. Fuchs, M. Podda and L. Packer, Marcel Dekker, Inc., New York, 2003, ch. 8, pp. 145–192.
4 C. Decarroz, J. R. Wagner, J. E. van Lier, C. M. Krishna, P. Riesz and J. Cadet, *Int. J. Radiat. Biol.*, 1986, **50**, 491–505.
5 C. M. Krishna, C. Decarroz, J. R. Wagner, J. Cadet and P. Riesz, *Photochem. Photobiol.*, 1987, **46**, 175–182.
6 C. Bienvenu, J. R. Wagner and J. Cadet, *J. Am. Chem. Soc.*, 1996, **118**, 11406.
7 A. Romieu, S. Bellon, D. Gasparutto and J. Cadet, *Org. Lett.*, 2000, **2**, 1085–1088.
8 Q. Zhang and Y. Wang, *J. Am. Chem. Soc.*, 2003, **125**, 12795–12802.
9 Q. Zhang and Y. Wang, *Nucleic Acids Res.*, 2005, **33**, 1593–603.
10 S. Bellon, J.-L. Ravanat, D. Gasparutto and J. Cadet, *Chem. Res. Toxicol.*, 2002, **15**, 598–606.
11 H. Hong, H. Cao, Y. Wang and Y. S. Wang, *Chem. Res. Toxicol.*, 2006, **19**, 614–621; Y. Jiang, H. Hong, H. Cao and Y. Wang, *Biochemistry*, 2007, **46**, 12757–12763.
12 C. Gu and Y. Wang, *Biochemistry*, 2005, **44**, 8883–8889.
13 S. Bellon, D. Gasparutto, C. Saint-Pierre and J. Cadet, *Org. Biomol. Chem.*, 2006, **4**, 3831–3837.
14 C. Gu, Q. Zhang, Z. Yang, Y. Wang, Y. Zou and Y. Wang, *Biochemistry*, 2006, **45**, 10739–10746.
15 B. Xerri, C. Morell, A. Grand, J. Cadet, P. Cimino and V. Barone, *Org. Biomol. Chem.*, 2006, **4**, 3986–3992.
16 M. J. Frisch, G. W. Trucks, H. B. Schlegel, G. E. Scuseria, M. A. Robb, J. R. Cheeseman, J. A. Montgomery, Jr., T. Vreven, K. N. Kudin, J. C. Burant, J. M. Millam, S. S. Iyengar, J. Tomasi, V. Barone, B. Mennucci, M. Cossi, G. Scalmani, N. Rega, G. A. Petersson, H. Nakatsuji, M. Hada, M. Ehara, K. Toyota, R. Fukuda, J. Hasegawa, M. Ishida, T. Nakajima, Y. Honda, O. Kitao, H. Nakai, M. Klene, X. Li, J. E. Knox, H. P. Hratchian, J. B. Cross, V. Bakken, C. Adamo, J. Jaramillo, R. Gomperts, R. E. Stratmann, O. Yazyev, A. J. Austin, R. Cammi, C. Pomelli, J. Ochterski, P. Y. Ayala, K. Morokuma, G. A. Voth, P. Salvador, J. J. Dannenberg, V. G. Zakrzewski, S. Dapprich, A. D. Daniels, M. C. Strain, O. Farkas, D. K. Malick, A. D. Rabuck, K. Raghavachari, J. B. Foresman, J. V. Ortiz, Q. Cui, A. G. Baboul, S. Clifford, J. Cioslowski, B. B. Stefanov, G. Liu, A. Liashenko, P. Piskorz, I. Komaromi, R. L. Martin, D. J. Fox, T. Keith, M. A. Al-Laham, C. Y. Peng, A. Nanayakkara, M. Challacombe, P. M. W. Gill, B. G. Johnson, W. Chen, M. W. Wong, C. Gonzalez and J. A. Pople, *GAUSSIAN 03 (Revision C.02)*, Gaussian, Inc., Wallingford, CT, 2004.
17 A description of basis sets and standard computational methods can be found in *Exploring Chemistry with Electronic Structure Methods*, 2nd edn, ed. J. B. Foresman and A. E. Frisch, Gaussian Inc., Pittsburg, PA, 1996.
18 F. Jolibois, A. Grand, J. Cadet, C. Adamo and V. Barone, *Chem. Phys. Lett.*, 1999, **301**, 255.
19 W. Kock and W. C. Holthousen, *A Chemist's Guide to Density Functional Theory*, Wiley-VCH, Weinheim, 2000.
20 R. G. Pearson, *J. Chem. Educ.*, 1986, **45**, 981.
21 C. Morell, A. Grand and A. Toro-Labbé, *J. Phys. Chem. A*, 2005, **109**, 205.
22 C. Morell, A. Grand and A. Toro-Labbé, *Chem. Phys. Lett.*, 2006, **425**, 342.
23 The $\Delta f(r)$ descriptor is calculated in the frozen core approximation by using the formula $\Delta f(r) = |\phi_{\mathrm{LUMO}}(r)|^2 - |\phi_{\mathrm{HUMO}}(r)|^2$.